



UvA-DARE (Digital Academic Repository)

A jet model for the broadband spectrum of XTE J1118+480. Synchrotron emission from radio to X-rays in the

Markoff, S.B.; Falcke, H.D.; Fender, R.P.

Publication date
2001

Published in
Astronomy & Astrophysics

[Link to publication](#)

Citation for published version (APA):

Markoff, S. B., Falcke, H. D., & Fender, R. P. (2001). A jet model for the broadband spectrum of XTE J1118+480. Synchrotron emission from radio to X-rays in the. *Astronomy & Astrophysics*, 372, 25.

General rights

It is not permitted to download or to forward/distribute the text or part of it without the consent of the author(s) and/or copyright holder(s), other than for strictly personal, individual use, unless the work is under an open content license (like Creative Commons).

Disclaimer/Complaints regulations

If you believe that digital publication of certain material infringes any of your rights or (privacy) interests, please let the Library know, stating your reasons. In case of a legitimate complaint, the Library will make the material inaccessible and/or remove it from the website. Please Ask the Library: <https://uba.uva.nl/en/contact>, or a letter to: Library of the University of Amsterdam, Secretariat, Singel 425, 1012 WP Amsterdam, The Netherlands. You will be contacted as soon as possible.

A jet model for the broadband spectrum of XTE J1118+480

Synchrotron emission from radio to X-rays in the Low/Hard spectral state

S. Markoff^{1,*}, H. Falcke¹, and R. Fender²

¹ Max-Planck-Institut für Radioastronomie, Auf dem Hügel 69, 53121 Bonn, Germany

² Astronomical Institute “Anton Pannekoek” and Center for High Energy Astrophysics, University of Amsterdam, Kruislaan 403, 1098 SJ Amsterdam, The Netherlands

Received 9 February 2001 / Accepted 21 March 2001

Abstract. Observations have revealed strong evidence for powerful jets in the Low/Hard states of black hole candidate X-ray binaries. Correlations, both temporal and spectral, between the radio – infrared and X-ray bands suggest that jet synchrotron as well as inverse Compton emission could also be significantly contributing at higher frequencies. We show here that, for reasonable assumptions about the jet physical parameters, the broadband spectrum from radio through X-rays can be almost entirely fit by synchrotron emission. We explore a relatively simple model for a relativistic, adiabatically expanding jet combined with a truncated thermal disk conjoined by an ADAF, in the context of the recently discovered black hole binary XTE J1118+480. In particular, the X-ray power-law emission can be explained as optically thin synchrotron emission from a shock acceleration region in the innermost part of the jet, with a cutoff determined by cooling losses. For synchrotron cooling-limited particle acceleration, the spectral cutoff is a function only of dimensionless plasma parameters and thus should be around a “canonical” value for sources with similar plasma properties. It is therefore possible that non-thermal jet emission is important for XTE J1118+480 and possibly other X-ray binaries in the Low/Hard state.

Key words. X-rays: binaries – X-rays: individual: XTE J1118+480 – radiation mechanisms: non-thermal – stars: winds, outflows – black hole physics – accretion, accretion disks

1. Introduction

Observations are providing increasing evidence that black hole candidate (BHC) X-ray binaries (XRBs) produce powerful collimated outflows when in the Low/Hard X-ray state (LHS). This state is characterized by a non-thermal power-law in the X-ray band and little, if any, thermal disk contribution (e.g., Nowak 1995; Poutanen 1998). At least three systems in the LHS (Cyg X-1, 1E 1740.7-2942 and GRS 1758-258) have directly resolved radio jets on scales from AU to parsecs. However, XRB jets also reveal themselves in the broadband LHS spectra with a flat-to-inverted radio synchrotron spectrum, analogous to the signature emission of jets in compact radio cores of AGN (Blandford & Königl 1979; Hjellming & Johnston 1988; Falcke & Biermann 1999). Furthermore, new data suggest a continuation of this radio synchrotron emission to much higher frequencies. The spatial, spectral and temporal evidence for powerful jets from XRB BHCs in the LHS are compiled and discussed in Fender (2001).

We know that jets play a significant role in the emission of Active Galactic Nuclei (AGN), even dominating

the spectrum from radio through TeV γ -rays in the case of BL Lacs, with emission from optically thin synchrotron up to even 100 keV and higher (e.g. Pian et al. 1998). By analogy, if the flat, optically thick synchrotron spectrum in XRBs, commonly attributed to jets, indeed extends into the NIR and optical regimes (Fender 2001), one would expect a corresponding optically thin power-law from shock acceleration at even higher frequencies. This is irrespective of whether the jet emission is boosted or not, since optically thick and optically thin emission would have similar Doppler factors. Shock acceleration is likely to be present in XRBs, given that optically thin power-law spectra are observed during their radio outbursts (e.g., Fender & Kuulkers 2001, and references therein).

Still, the majority of current models for the broadband (X-ray) spectra of BHC XRBs focus only on the contribution of thermal disk plus coronal inverse Compton (IC) emission (for a review, see Poutanen 1998) and ignore any jet contribution, even though jets can be an integral part of X-ray binaries and their systems (e.g., Eikenberry et al. 1998; Mirabel & Rodríguez 1999; Fender 2001).

As an example for the possible importance of jet emission, we use the recently discovered XRB XTE J1118+480 (Remillard et al. 2000), which has been observed in the radio through X-rays (see Hynes et al. 2000, hereafter H00;

Send offprint requests to: S. Markoff,
e-mail: smarkoff@mpifr-bonn.mpg.de

* Humboldt research fellow.

Fender et al. 2001, hereafter F01, and references therein), and is also at high enough Galactic latitude to allow the first ever EUV detections of an X-ray transient (H00). The system is likely a BHC in the LHS (H00; Revnivtsev et al. 2000; Wood et al. 2000). Although jets were not directly resolved with MERLIN to a limit of $< 65(d/\text{kpc})$ AU (at 5 GHz; F01), its radio emission shows the flat characteristic jet spectrum.

2. Basic model and estimates

We consider that an accretion disk is responsible for the extreme-ultraviolet (EUV) data and contributes in the optical (H00; Garcia et al. 2000). However, the power-law seen in the X-ray spectrum indicates that an additional component must be present. So far, this has been presumed to arise from the Comptonization of some “seed” photons by a hot, thermal corona (Poutanen 1998).

One commonly invoked physical explanation for the LHS is that a standard thin, optically thick disk (Shakura & Sunyaev 1973) exists only down to some transition radius $r_{\text{tr}} \sim 10^2 - 10^3 r_s$, ($r_s = 2GM_{\text{bh}}/c^2$), where the flow becomes hot and non-radiative (e.g., Liu et al. 1999; Esin et al. 2001). We do not, however, include an entire disk model here, since there are several models already in existence exploring this issue (see above, and review in Poutanen 1998). Instead, we include a representative thermal spectrum for the inner edge of the cool disk both in the direct emission, in our calculations of cooling rates in the jet and as seed photons for IC.

With this approach the temperature, T_d , and luminosity, L_d , for this inner edge can be roughly determined by fitting a black body to the EUV data. As discussed in H00, uncertainty in the local absorption leads to large variations in the possible EUV flux for XTE J1118+480. Here, we take the highest absorption value presented, $N_{\text{H}} = 1.15 \times 10^{20} \text{ cm}^{-2}$, because it provides a solid upper limit to any thermal disk contribution (see Fig. 1).

Taking the distance and BH mass to be 1.8 kpc and $6 M_{\odot}$, respectively (McClintock et al. 2001a), the fit to the EUV data gives $T_d \sim 1.5 \times 10^5 \text{ K}$ and $L_d \sim 5 \times 10^{35} \text{ erg s}^{-1}$. For an annulus with scale width $\sim r_{\text{tr}}$, we find as an order of magnitude estimate $r_{\text{tr}} \approx 900 r_s$, in agreement with current models (e.g., Liu et al. 1999). The luminosity of a standard accretion disk is dominated by the inner edge and its radiative efficiency is $q_1 = \frac{1}{4} r_s / r_{\text{tr}}$ (Frank et al. 1992, Eq. (5.20)), yielding a rough estimate for the accretion rate of $\dot{M}_d \sim q_1^{-1} L_d / c^2 \simeq 3 \times 10^{-8} M_{\odot} \text{ yr}^{-1}$. Hence, in the following we use a reference value of $\dot{M}_d = \dot{m}_{-7.5} 3 \times 10^{-8} M_{\odot} \text{ yr}^{-1}$. Within r_{tr} we consider a hot, ADAF-like flow which does not significantly contribute to the spectrum.

For accreting black holes it has been argued that the jet power is of order $Q_{\text{jet}} \sim q_j \dot{M}_d c^2$ with an efficiency inferred to be of order $q_j = 10^{-1} - 10^{-3}$ (Falcke & Biermann 1999). However, q_j is essentially a free parameter, with $q_j \ll 1$, and we define $q_{j,-2} = q_j / 10^{-2}$. While the jet formation itself is very difficult to model, the physics of calculating

most of the jet emission is relatively straightforward because the flat-to-inverted spectrum stems from the part of the jet where it is basically undergoing free expansion. Here we build on the jet emission model outlined in Falcke & Markoff (2000), and references therein.

At the inner edge of the hot accretion flow, plasma is ejected out from symmetric nozzles, where it becomes supersonic. The jets then accelerate along the axes through their pressure gradients up to bulk Lorentz factors $\gamma_j \simeq 2-3$, and expand sideways with their initial proper sound speed $\gamma_s \beta_s c \simeq 0.4c$ for a hot electron/proton plasma. This implies low relativistic Mach numbers around $\mathcal{M} \sim 5$. The velocity field, density and magnetic field gradient then come naturally from the Euler equation (see, e.g., Falcke 1996). The dependencies of the magnetic field B and density n on distance are then similar to, but slightly stronger than, the canonical r^{-1} and r^{-2} dependencies for conical jets, respectively (Blandford & Königl 1979; Hjellming & Johnston 1988; Falcke & Biermann 1995).

In this way, the basic physical properties governing the emission at each point in the jet are fixed after specifying the jet power, and the initial conditions at the nozzle. We make the simplification of assuming a maximal jet, which follows from the Bernoulli equation (Falcke & Biermann 1995) when the internal energy, here dominated by the magnetic field, is equal to the bulk kinetic energy of particles. This is consistent with a magnetic launching mechanism. The plasma is assumed to originate in the hot accretion flow and therefore contains equal numbers of protons and electrons, with hot electrons at a temperature approaching $T_e = T_{e,10} \times 10^{10} \text{ K}$ in various ADAF models (e.g., Manmoto 2000). The electron Lorentz factor of the peak will be at $\gamma_e \sim 4 \cdot T_{e,10}$.

In AGN jets, the high frequency, optically-thin power-laws are taken to be the result of synchrotron emission from particles being shock-accelerated along the jet (e.g., Marscher & Gear 1985). In such a case the crucial parameter for the high energy emission is the location z_{acc} of the first particle acceleration region in the jet.

Near the shock region in each jet, $B^2(r)/8\pi \simeq 0.25 q_j \dot{M}_d c^2 / (c \gamma_j \beta_j \pi r^2)$, yielding a reference value of $B \simeq 2 \times 10^6 \text{ G} \cdot \sqrt{q_{j,-2} \dot{m}_{-7.5} / \gamma_j \beta_j} (r/10r_s)^{-1}$ for the parameters discussed above. Similarly, the particle density is given by $n \simeq 10^{14} \text{ cm}^{-3} \cdot (q_{j,-2} \dot{m}_{-7.5} / \gamma_j \beta_j) (r/10r_s)^{-2}$.

Once the plasma, assumed to be injected at the base of the jet with a Maxwellian distribution, reaches the shock region, the standard diffusive shock acceleration process redistributes the particles into a power-law, starting roughly at $\gamma_{e,\text{min}} \sim 4T_{e,10}$. The initially injected distribution has an index $p \simeq 1.5-2$ (resulting from a relativistic shock, see, e.g., Heavens & Drury 1988¹) steepening by ~ 1 due to increased cooling above a break

¹ Because the plasma is mildly relativistic at the shock region, the temperature-dependent adiabatic index will be closer to 4/3 rather than the non-relativistic value of 5/3. This yields a spectral index of $1.5 \lesssim p \leq 2$, where $p = 2$ is for non-relativistic shock-acceleration.

energy $E_b \approx (\tau_r \beta_{\text{cool}})^{-1}$, where τ_r is the residence time of the plasma in the acceleration region, and β_{cool} are the constants giving the energy dependence of the cooling, which for synchrotron and Compton losses go as $\dot{E} \approx -\beta_{\text{cool}} E^2$. This steepened spectrum has the index of $p \simeq 2.5\text{--}3$, typically found in the optically thin synchrotron emission of both AGN and X-ray binaries. For the case of XTE J1118+480, the unbroken X-ray power-law (see Fig. 1), implies $p \simeq 2.6$ for $E > E_b$. The acceleration ceases when the particles reach the energy $E_{e,\text{max}} = \gamma_{e,\text{max}} m_e c^2$ where the cooling/loss rates equal that of acceleration. These rates are dependent both on the energy of the particle, as well as the local physical parameters.

The shock acceleration rate is given as

$$t_{\text{acc}}^{-1} = \frac{3}{4} \left(\frac{u_{\text{sh}}}{c} \right)^2 \frac{eB}{m_e c \xi \gamma_e}, \quad (1)$$

where u_{sh} is the shock speed in the plasma frame. The parameter $\xi < c\beta_e/u_{\text{sh}}$ (Jokipii 1987) is the ratio between the diffusive scattering mean free path and the gyroradius of the particle, and has a lower limit at $\xi = 1$. We account for energy losses at the shock via adiabatic losses, particle escape, IC and synchrotron. In our case the latter dominates and we have

$$t_{\text{syn}}^{-1} = \frac{4}{3} \sigma_T \gamma_e \beta_e^2 \frac{U_B}{m_e c} \quad (2)$$

where σ_T is the Thomson cross-section and U_B is the energy density of the magnetic field. The maximum energy is then found by solving $t_{\text{acc}}^{-1} = t_{\text{syn}}^{-1}$, yielding $\gamma_{e,\text{max}} \sim 10^8 (\xi B)^{-0.5} \left(\frac{u_{\text{sh}}}{c} \right)$. If we define as a reference value $\xi = \xi_2 100$, the maximum synchrotron frequency is

$$\nu_{\text{max}} = 0.29 \nu_c \simeq 1.2 \times 10^{20} \xi_2^{-1} \left(\frac{u_{\text{sh}}}{c} \right)^2 \text{ Hz} \quad (3)$$

where $\nu_c \simeq \frac{3}{4\pi} \gamma_{e,\text{max}}^2 (eB)/(m_e c)$ is the critical synchrotron frequency. This maximum corresponds approximately to the rollover of the power-law cutoff, and for $u_{\text{sh}} \sim \beta_s c$, we find a cutoff of ~ 80 keV. This cutoff is not dependent on the magnetic field, the jet power, or the shock location as long as we are in the synchrotron cooling dominated regime. Because we would expect XRBs to have similar shock structures, once ξ is roughly fixed observationally – thus determining the scattering between magnetic irregularities in the diffusive shock process – we should get similar cutoffs for different sources and accretion rates.

The location of the initial shock acceleration region is set by the frequency where the flat, highly self-absorbed synchrotron spectrum turns over into the optically thin power-law produced at the shock. From back-extrapolating the X-ray power-law, we can see that this maximum self-absorption frequency has to be somewhere in the IR/optical regime at $\sim 10^{14.5}$ Hz. For the parameters discussed here this would be at a distance of roughly $z_{\text{acc}} \simeq 50 r_s$, with a jet radius of $r \simeq 10 r_s$, and the magnetic field and particle densities derived above. The

total synchrotron luminosity, integrated up to the highest energies, is a few times 10^{36} erg s^{-1} , which is $\sim 10\%$ of the total jet power ($Q_j \sim q_{j,-2} \dot{m}_{-7.5} 2 \times 10^{37}$ erg s^{-1}).

Some fraction of X-rays created close to the nucleus by the jet will of course either directly impinge on, or be scattered by hot electrons into, the cold disk, resulting in a reflection component. However, since this is very dependent on the disk geometry, and because the feature is very weak or absent for XTE J1118+480 (McClintock et al. 2001b), we do not calculate this process here.

3. Results of numerical modeling

To obtain a more detailed broadband spectrum we have used the full numerical calculations for a jet model as described in Falcke & Markoff (2000), with the addition of a particle acceleration region. The model takes into account the relativistic Doppler shifts, adiabatic losses, electron acceleration and loss timescales at the acceleration region as described above, and integrates the synchrotron and IC emission along the jet. The resulting fit is shown in Fig. 1 with the parameters given in the caption.

The relevant free parameters are the inclination angle θ_i , the shock distance z_{acc} , the scattering ratio ξ , and the jet power parameterized by q_j . While the electron temperature T_e (or $\gamma_{e,\text{min}}$) and the fraction of thermal particles accelerated can also be adjusted, they are not independent of q_j – decreasing these parameters will decrease the radiative efficiency and increase q_j . Similarly, a more realistic disk model (e.g., Esin et al. 2001) could yield a lower r_{tr} and \dot{M} , also increasing q_j . Because we require charge balance between protons and electrons for the jet plasma, and a low T_e in line with ADAF models, the particles are in sub-equipartition with the magnetic field.

The flat spectrum from radio to optical is due to the optically thick synchrotron emission from the jet at $z > z_{\text{acc}}$, while the X-ray power-law is the optically thin synchrotron emission dominated by the shock acceleration region (at $z \sim z_{\text{acc}}$). For the conditions in the jet, E_b lies very close to the peak of the thermal electron distribution, and we only see the steepened power-law. Because of the large ratio between magnetic field and photon densities, IC emission does not play a significant role for the parameters chosen here (see Fig. 1). Synchrotron and IC emission from the pre-shock region ($z < z_{\text{acc}}$) could in principle show up in the soft and very hard X-rays respectively as a function of T_e , but the EUV points place an effective upper limit $T_e \lesssim 2 \times 10^{10}$ K, and so for this source these features are rather weak.

The jet length may be constrained by the turnover seen in the $\sim 2\text{--}15$ GHz range, which gives a length of $\sim 4 \times 10^{13}$ cm, i.e. ~ 1.5 mas (at 1.8 kpc), in the GHz range with a $\nu^{-0.9}$ scaling of the size (Falcke 1996).

The optically thin synchrotron power-law component in the X-rays depends on the existence of a diffusive shock acceleration region. The current limit on γ_e comes from synchrotron losses instead of IC, due to the weak disk emission, which results in a low external photon density.

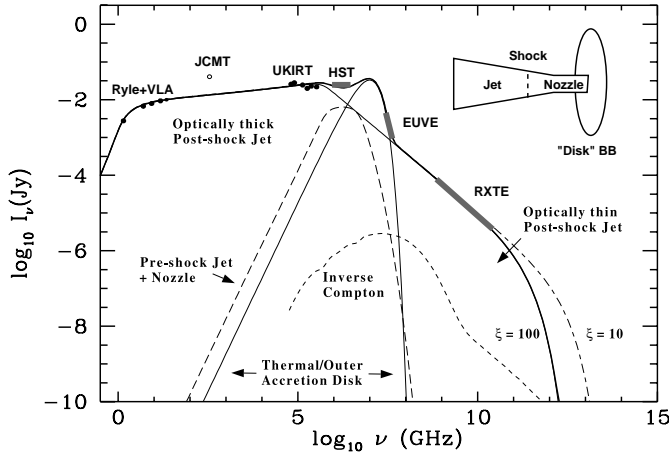


Fig. 1. Fit to data from H00, with the exception of the VLA radio points (Hjellming et al., private comm.), the Ryle Telescope and a non-simultaneous JCMT point (see F01, and refs. therein). Included is a schematic indicating the different emission components. Parameters are $M_{\text{bh}} = 6 M_{\odot}$, $r_{\text{nozz}} = 1.5r_s$, $T_d = 1.7 \times 10^5$ K, $L_d = 5.25 \times 10^{35}$ ergs s^{-1} , $\dot{m} = 0.1$, $L_j = 2.6 \times 10^{36}$ erg s^{-1} , $r_{\text{tr}} = 747r_s$, $q_{j,-2} = 1.5$, $\xi_2 = 1$, $z_{\text{acc}} = 45r_s$, $\theta_i = 32^\circ$. The fraction of thermal particles accelerated at the shock was fixed at 50%. The dot-dashed line shows the cutoff for the case of $\xi_2 = 0.1$.

In this case, the location of the X-ray cutoff is determined by ξ and is fit observationally, keeping in mind that ξ is typically under a few 10^2 (e.g., Jokipii 1987). A “canonical” cutoff at ~ 100 keV (e.g., Poutanen 1998) corresponds to $\xi \sim 100$, and $\nu_{\text{max}} \propto \xi^{-1}$. We also plot both $\xi = 10$ and $\xi = 100$ in Fig. 1, in order to illustrate how the cutoff could theoretically venture into the realm of future high-energy missions like INTEGRAL with energies \lesssim a few MeV. For XTE J1118+480, such a high cutoff may be necessary, as McClintock et al. (2001b) see no cutoff below ~ 160 keV.

4. Conclusion

From our modeling we conclude that in the LHS of XTE J1118+480 a significant jet contribution from radio through IR is present, and with reasonable assumptions and a small efficiency could extend even up to the hard X-rays. We cannot exclude that XTE J1118+480, with its rather low luminosity, is a special source. However, our model is scalable and thus likely applicable to other XRBs in the LHS, when a flat radio spectrum is present.

An important element of the model is that the inner ADAF-like flow is very hot and radiatively inefficient, injecting (mildly) relativistic electrons into the jet and allowing high electron energies because of low IC cooling. With a more dominant disk contribution, e.g., in the High/Soft state, the jet spectrum would also change and possibly disappear due to increased cooling. Interestingly, in the case of a low disk contribution, synchrotron-dominated cooling provides a natural “canonical” cutoff

around 100 keV, which only depends on the dimensionless plasma parameters ξ and u_{sh}/c . Small variations in the spectral index of the synchrotron power-law could explain the observed time lags in some sources (Kotov et al. 2001). The jet model for XTE J1118+480 may therefore provide an interesting new perspective for the modeling of XRBs in general.

Acknowledgements. We thank P. L. Biermann, M. Nowak, T. Beckert and the referee for useful discussions and comments. We are very appreciative of data made available to us by R. Hjellming shortly before his untimely death.

References

- Blandford, R. D., & Königl, A. 1979, *ApJ*, 232, 34
 Eikenberry, S. S., Matthews, K., Morgan, E. H., Remillard, R. A., & Nelson, R. W. 1998, *ApJ*, 494, L61
 Esin, A. A., McClintock, J. E., Drake, J. J., et al. 2001, *ApJ*, in press [astro-ph/0103044]
 Falcke, H. 1996, *ApJ*, 464, L67
 Falcke, H., & Biermann, P. L. 1995, *A&A*, 293, 665
 Falcke, H., & Biermann, P. L. 1999, *A&A*, 342, 49
 Falcke, H., & Markoff, S. 2000, *A&A*, 362, 113
 Fender, R. P. 2001, *MNRAS*, 322, 31
 Fender, R. P., Hjellming, R. M., Tilanus, R. J., et al. 2001, *MNRAS*, 322, L32
 Fender, R. P., & Kuulkers, E. 2001, *MNRAS*, in press [astro-ph/0101155]
 Frank, J., King, A., & Raine, D. 1992, *Accretion Power in Astrophysics* (Cambridge University Press), 1992.
 Garcia, M., Brown, W., Pahre, M., et al. 2000, *IAU Circ.*, 7392
 Heavens, A. F., & Drury, L. O. 1988, *MNRAS*, 235, 997
 Hjellming, R. M., & Johnston, K. J. 1988, *ApJ*, 328, 600
 Hynes, R. I., Mauche, C. W., Haswell, C. A., et al. 2000, *ApJ*, 539, L37 (H00)
 Jokipii, J. R. 1987, *ApJ*, 313, 842
 Kotov, O., Churazov, E., & Gilfanov, M. 2001, *MNRAS*, submitted [astro-ph/0103115]
 Liu, B. F., Yuan, W., Meyer, F., Meyer-Hofmeister, E., & Xie, G. Z. 1999, *ApJ*, 527, L17
 Manmoto, T. 2000, *ApJ*, 534, 734
 Marscher, A. P., & Gear, W. K. 1985, *ApJ*, 298, 114
 McClintock, J. E., Garcia, M. R., Caldwell, N., et al. 2001a, *ApJ*, in press [astro-ph/0101421]
 McClintock, J. E., Haswell, C. A., Garcia, M. R., Drake, J. J., & Hynes, R. 2001b, *ApJ*, submitted [astro-ph/0103051]
 Mirabel, I. F., & Rodríguez, L. F. 1999, *ARA&A*, 37, 409
 Nowak, M. A. 1995, *PASP*, 107, 1207
 Pian, E., Vacanti, G., Tagliaferri, G., et al. 1998, *ApJ*, 492, L17
 Poutanen, J. 1998, in *Theory of Black Hole Accretion Disks* (Cambridge University Press), 100
 Remillard, R., Morgan, E., Smith, D., & Smith, E. 2000, *IAU Circ.*, 7389
 Revnivtsev, M., Sunyaev, R., & Borozdin, K. 2000, *A&A*, 361, L37
 Shakura, N. I., & Sunyaev, R. A. 1973, *A&A*, 24, 337
 Wood, K. S., Ray, P. S., Bandyopadhyay, R. M., et al. 2000, *ApJ*, 544, L45